Incorporation of an indole-3 butyric acid modified clay in epoxy resin for corrosion protection of carbon steel

Trinh Anh Truc [a], To Thi Xuan Hang [a], Vu Ke Oanh [a], Eric Dantras [b], Colette Lacabanne [b], Djar Oquab [c], Nadine Pébère [c],*

[a] Laboratory for Protective Coatings, Institute for Tropical Technology, 18 Hoang Quoc Viet, Hanoi, Vietnam
[b] Centre Interuniversitaire de Recherche et d'Ingénierie des Matériaux (CIRIMAT) Laboratoire de Physique des Polymères, UMR CNRS 5085, Université Paul Sabatier, 118, Route de Narbonne - 31062 Toulouse cedex 04, France
[c] CIRIMAT/UMR CNRS 5085, ENSIACET, 118, Route de Narbonne - 31077 Toulouse cedex 04, France

ARTICLE INFO

ABSTRACT

In the present work, indole-3 butyric acid (IBA) was inserted between montmorillonite clay platelets by cation exchange. The clay treated with the organic compound (IBA-modified clay) was then dispersed in an epoxy resin at a low concentration (2 wt.%). IBA was chosen to act both as an inhibitor and an adherence promoter. The effect of the IBA-modified clay on the microstructure and on the protective properties of the epoxy coating deposited on carbon steel was evaluated by a thermostimulated-current (TSC) method and by electrochemical impedance spectroscopy (EIS). The TSC measurements showed the specific action of IBA-modified clay which decreased the molecular mobility of the polymer chain by comparison with the pure epoxy. Impedance measurements corroborated the role of the modified clay on the barrier properties of the coating which remained high as a function of exposure time in a 0.5 M NaCl solution. The corrosion resistance of the carbon steel coated with the epoxy resin containing IBA-modified clay was significantly higher than that obtained with the clear coat. Polarization curves plotted in the presence of an artificial defect demonstrated the inhibitive role of IBA at the carbon steel/coating interface. The good adherence of the coating was seen during salt spray test.

© 2008 Elsevier B.V. All rights reserved.

1. Introduction

Organic coatings are widely used to prevent corrosion of metallic structures because they can easily be applied at a reasonable cost. It is generally accepted that the coating efficiency is dependent on the intrinsic properties of the organic film (barrier properties), the substrate/coating interface in terms of adherence, the inhibitive or sacrificial pigments included in the primer and the degree of environment aggressiveness. Due to the problems of high toxicity associated with inhibitive pigments such as strontium or zinc chromates, various studies have been carried out to develop more acceptable environmentally coatings.

Although there are numerous non-toxic organic compounds that are excellent corrosion inhibitors in solution such as amines, phosphonic acids, carboxylic acids or heterocyclic compounds [1–5], these materials have not yet found widespread applications in protective organic coatings. The reason for their lack of use is that the active part of the compounds ($-NH_2$, $-POOH$, $-COOH$), which is responsible for the inhibitive effect (formation of strong bonds with the metal surface) can also, unfortunately, react with the polymer resins used to produce the coating. Thus, the corrosion inhibitor is trapped by the polymer chain, and cannot diffuse through the coating to reach the metal/film interface to prevent corrosion reactions. In addition, most of these organic inhibitors are soluble in water. This could cause blistering of the coatings when they are in contact with moisture. One way to solve these problems is to attach the inhibitor molecules to a clay backbone and to disperse the organically modified clay in the coating. The inhibitors could then be slowly released at the metal/coating interface and react with the substrate [6–10].

In a previous work [11], montmorillonite clay (MMT) treated with aminotrimethyl-phosphonic acid (ATMP) and dispersed in an epoxy resin was used to improve the corrosion protection of carbon steel. The clay modified by ATMP (ATMP-modified clay) was prepared by cation exchange reaction. It was shown that the presence of ATMP-modified clay significantly enhanced the protective properties of the epoxy coating. The corrosion protection in the presence of ATMP-modified clay was explained by both the barrier properties due to the lamellar structure of the clay and the corrosion inhibition at the carbon steel surface due to the presence of phosphonic functions in the organic molecule. However, it was seen that adhesion of the coating was not better than with pure epoxy, significant delamination being observed. Good coating adherence is required to develop an efficient protective primer.

* Corresponding author. Fax: +33 5 62 88 56 63.
E-mail address: nadine.pebere@ensiacet.fr (N. Pébère).

The aim of the present study is to propose a new organic compound which will be both a corrosion inhibitor and an adherence promoter. For this purpose, indole-3 butyric acid (IBA) was chosen to replace ATMP within the MMT platelets. It was shown [12] that IBA tested in a 0.5 M NaCl solution, as a corrosion inhibitor, presented a good efficiency and can be classified as an anodic inhibitor. The action of IBA was attributed to the chemisorption of the organic compound onto the steel surface. The rigid structure of IBA is assumed to improve the film adherence.

As in the previous study [11], MMT was treated with IBA (IBA-modified clay) by cation exchange. The IBA-modified clay was first characterized by infrared spectroscopy and thermogravimetric analysis. To verify the dispersion of the IBA-modified clay in the epoxy resin, the fracture surface of the coating was observed by Field-Emission Scanning Electron Microscope (FE-SEM). The effect of the IBA-modified clay on the microstructure of the coating was characterized by a thermostimulated-current (TSC) method. Finally, the protective properties of the epoxy resin containing IBA-modified clay were monitored by electrochemical impedance measurements in a 0.5 M NaCl solution at different immersion times up to 140 days and compared with those of the pure epoxy resin. To determine the mode of action of the organic molecules at the steel/coating interface, an artificial defect was bored through the coating and polarization curves (anodic and cathodic plots) were obtained. Salt spray tests were performed to verify both the protection afforded by, and the adherence of, the system containing IBA-modified clay.

2. Experimental

2.1. Materials

Carbon steel sheets ($150 \times 10 \times 2$ mm) were used as substrates. They had the following composition in percent weight C=0.35, Mn=0.65, Si=0.25, P=0.035 and Fe to 100. They were polished with abrasive papers from 80 to 600 grade, washed by water and cleaned with ethanol.

Indole-3 butyric acid (IBA) was purchased from Sigma Aldrich. The chemical structure of IBA is shown in Fig. 1. The MMT was from Tuy Phong—Binh Thuan province in Vietnam. This clay consisted of a 2/1 ratio of silica to alumina, the swelling degree was 500% and the ion exchange capacity was 100–115 meq/100 g. Before use, the hydrophilic clay was rinsed with pure water and a homogeneous suspension obtained.

2.2. IBA modification of the clay

The pristine clay (3.0 g) was dispersed in distilled water (300 ml) containing concentrated hydrochloric acid (0.5 ml) and IBA (7.0 g). The concentration of IBA was chosen to be higher than the ion exchange capacity of the pristine clay (10 times higher). The suspension was stirred at 70 °C for 24 h to afford a white precipitate. This precipitate was filtered and washed with water until no chloride was detected in the filtrate using a 0.1 M AgNO$_3$ solution. The IBA-modified clay was then dried at 80 °C in a vacuum oven for 2 days.

2.3. Coating

The epoxy resin was Epon 828 and the hardener was Epikure 207. Both compounds were purchased from Herison Co. (Germany).
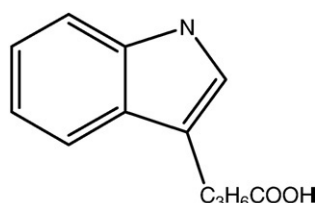

Fig. 1. Molecular structure of indole-3 butyric acid.

The IBA-modified clay was incorporated into the epoxy coating at a concentration of 2 wt.%. This concentration was chosen because in the previous work [11], the best corrosion protection was obtained with 2% clay content. An increase of the modified clay in the coating did not improve corrosion protection. This low clay content is sufficient to achieve the required properties [3–5].

The liquid paints (pure epoxy and epoxy resin containing IBA-modified clay) were applied by spin coating. After drying (ambient temperature for 24 h) the coating thickness was measured by a Minitest 600 Erichen digital meter.

For the impedance measurements, the films studied were 20 ± 3 μm thick. For FE-SEM observations and TSC measurements, the films were 30 ± 5 μm thick.

For the polarization measurements, an artificial defect was bored through the coating with a 0.35 mm diameter drill. The surface area of the defect, determined by optical microscopy, was equal to 0.07 mm^2.

2.4. Analytical characterizations

Fourier transform infrared spectra were recorded with a Nexus 670 Nicolet spectrometer over the range 4000 cm^{-1}–400 cm^{-1}. The spectra of clay, IBA and IBA-modified clay were recorded from a KBr disc.

Thermodegradation of the pristine clay and IBA-modified clay was determined through thermogravimetric analysis (TGA). The weight loss curves were obtained using a Setaram thermogravimetric analyzer. Experiments were performed in nitrogen atmosphere over a temperature range 20–700 °C with a 10 °C/min heating ramp.

TSC measurements were carried out with home-made equipment, previously described [13–16]. The principle of the technique is briefly: polymer coated on metal substrate is placed between two electrodes in a hermetic cell filled with dry helium. Thereafter, it is polarized with a DC field E_p during a given time t_p at the temperature T_p. The system, under the electric field, is then quenched till $T_0 \ll T_p$ by liquid nitrogen: the previously induced dipolar orientation is frozen. Then, the sample is short-circuited for a given time (t_{cc}) to evacuate surface charges. Finally, the temperature is increased from T_0 to a final temperature $T_f > T_p$, at a constant heating rate q and the depolarization current I due to the return to equilibrium of the dipolar units is recorded with a Keithley 642 electrometer with sensitivity of 10^{-16} A. The following parameters applied in the present study are: t_p=2 min, t_{cc}=2 min and q=7 °C/min. Temperatures T_p, T_0 and T_f were chosen according to the range of temperature in which the relaxation modes are observed.

FE-SEM observations were carried out using a JSM-6700F from JEOL.

2.5. Electrochemical characterizations

For the EIS measurements, a three-electrode cell was used: the working electrode with an exposed area of 28 cm^2, the saturated calomel reference electrode (SCE) and a platinum auxiliary electrode. The corrosive medium was a 0.5 M NaCl solution (reagent grade) in contact with air, quiescent and at ambient temperature. The electrochemical impedance measurements were performed using an Autolab PGSTAT30 over a frequency range of 100 kHz to 10 mHz with seven points per decade using 30 mV peak-to-peak sinusoidal voltage. EIS data were analyzed by Z-View software version 2.9. Anodic and cathodic polarization curves were obtained after 30 min of immersion at a scan rate of 1 mVs^{-1} starting from the corrosion potential. For the electrochemical measurements, three samples were tested to ensure reproducibility.

3. Results and discussion

First, IR spectroscopy and TG analysis are presented to show the chemical changes occurring in the IBA-modified clay and to evaluate the IBA content of the modified clay. Then, TSC and SEM results describe the changes of the epoxy coating microstructure induced by
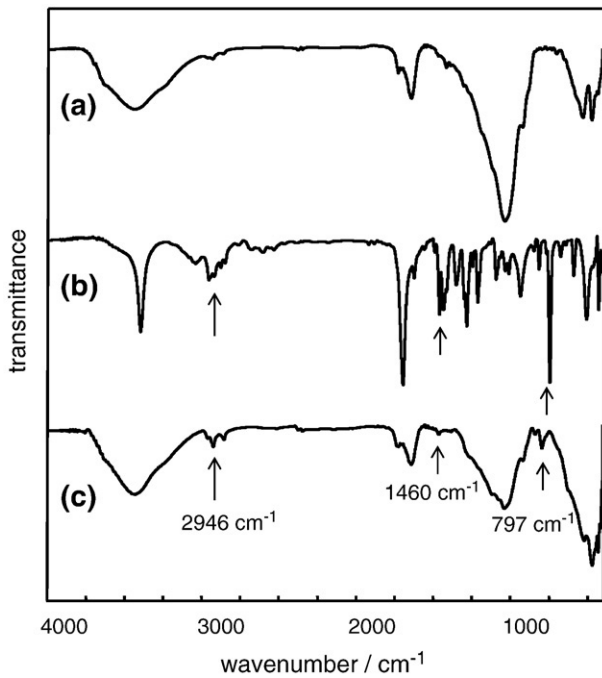
Fig. 2. FTIR spectra of (a) clay (MMT), (b) IBA and (c) IBA-modified clay.

the presence of IBA-modified clay. Finally, the corrosion protection of the carbon steel coated by the epoxy resin containing IBA-modified clay is discussed from the analysis of the electrochemical impedance data. To show the action of the IBA at the carbon steel/epoxy coating interface, polarization curves were plotted for the systems with an artificial defect. At the end, the electrochemical results were validated by salt spray tests.

3.1. Characterization of IBA-modified clay and epoxy containing IBA-modified clay

Fig. 2 presents the FTIR spectra of clay, IBA and IBA-modified clay. The characteristic bands of the spectra are given in Table 1. The spectrum of the clay shows bands at 1032 cm^{-1}, 524 cm^{-1} and 468 cm^{-1} characteristic of the Si–O, Al–O and Mg–O bonds, respectively [17]. These bands were also found in the spectrum of IBA-modified clay (1036 cm^{-1}, 526 cm^{-1} and 468 cm^{-1}). The hydrocarbon chain of IBA gave bands at 2946 cm^{-1}, 1460 cm^{-1} and 797 cm^{-1} and IBA-modified clay also presented the same bands. The band at 797 cm^{-1} for IBA and IBA-modified clay was attributed to the C–H bond in the aromatic ring [18]. From the comparison of the three spectra (Fig. 2), it can be concluded that the IBA molecules were inserted into the clay backbone.

Fig. 3 shows TGA thermograms for the clay and the IBA-modified clay. In Fig. 3a and b, each weight loss sigmoid is associated with a peak on −dw/dT curve. This representation allows us to follow with accuracy the evolution of weight sample as a function of temperature. Between 40 °C and 100 °C, the unmodified clay lost 10 wt.% which corresponds to the evaporation of water molecules present in the

Table 1
Characteristic bands of FTIR spectra obtained for IBA, clay and IBA-modified clay

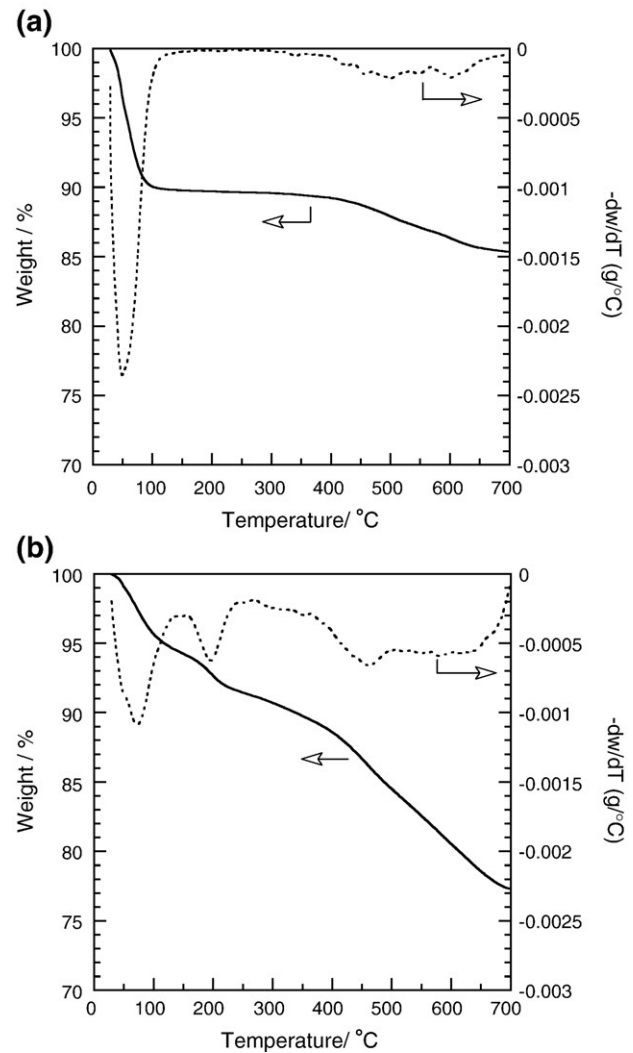| IBA	Clay	IBA-modified clay	Bond
(cm^{-1})	(cm^{-1})	(cm^{-1})	
–	468	468	Mg–O
–	524	526	Si–O–Al
–	1032	1036	Si–O
2946, 1460, 797	–	2946, 1460, 797	–CH$_2$

Fig. 3. Thermogravimetric spectra of (a) clay and (b) IBA-modified clay.

interlayers (Fig. 3a). Then, between 100 °C and 400 °C, the TG curve remains constant. This indicates that all the water had evaporated. Between 400 °C and 700 °C, an additional weight loss of about 4 wt.%
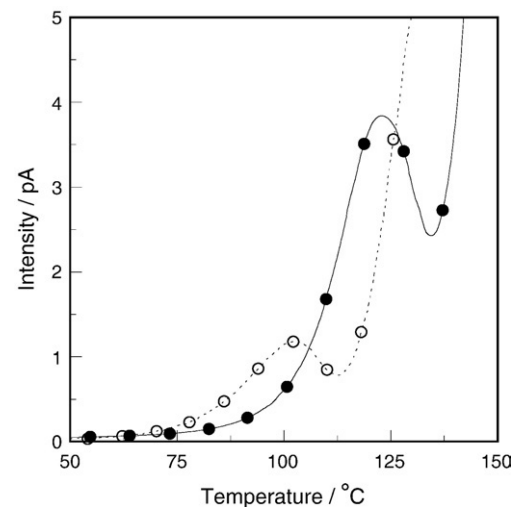

Fig. 4. TSC spectra of (—○—) pure epoxy coating and (—●—) epoxy coating containing 2 wt.% of IBA-modified clay.
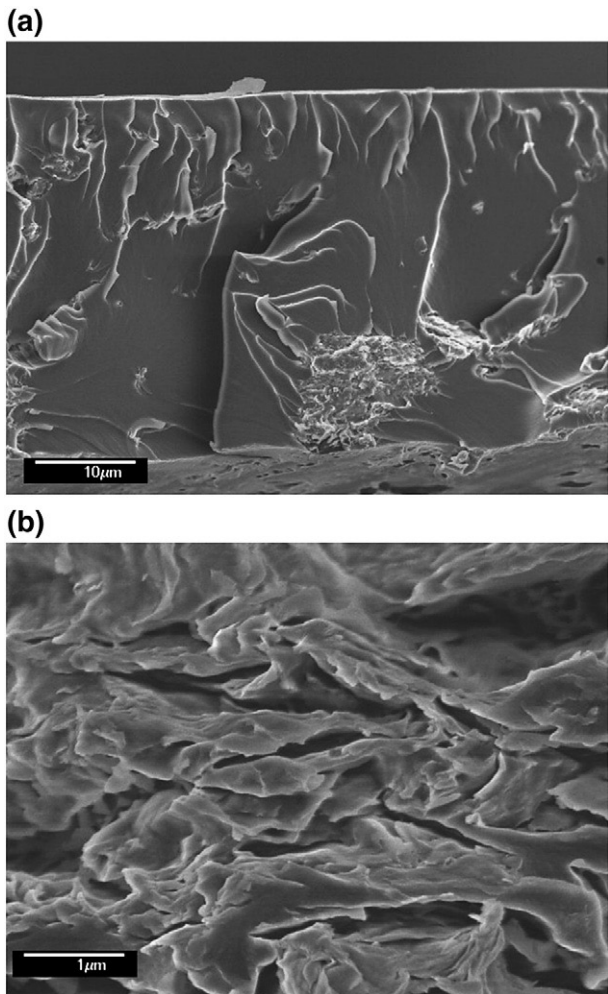
Fig. 5. FE-SEM micrograph of a fracture surface of epoxy coating containing 2 wt.% of IBA-modified clay. (a) ×2000 and (b) ×20,000.

was observed attributed to the dehydration of the remaining water within the crystal lattice [19,20]. For the IBA-modified clay thermogram (Fig. 3b), two plateaus are observed. The first one is the same as

that observed for the untreated clay but the weight loss is in this case lower (5 wt.%). The second plateau around 200 °C is attributed to the thermal decomposition of IBA (6 wt.%). Then, above 400 °C, the total dehydration of the system was again observed; however, the weight loss is higher than that previously measured (about 10%) and thus, it can be assumed that degradation of IBA molecules incorporated into the lattice could also occur in this temperature range. From the comparison of the two thermograms, it can be concluded that the modified clay contains about 10 wt.% of IBA.

The TSC spectra obtained for the pure epoxy and for the epoxy coating containing 2% IBA-modified clay are reported in Fig. 4. The TSC spectra exhibit a peak at 100 °C for the pure epoxy and at 120 °C for the epoxy containing IBA-modified clay. These peaks are associated to the dielectric manifestation of the glass transition temperature (T_g). The peak shift towards higher temperatures for the epoxy containing IBA-modified clay indicates a restriction of the molecular mobility of the organic chains in the presence of the IBA-modified clay due to interactions between the clay and the polymer molecules (additional cross-linking). In addition, specific electrostatic interactions between pigments (such as chromates) and the binder can enhance interactions and thus result in lower chain mobility (higher T_g) [15]. Here, electrostatic interactions between the clay and the epoxy coating can explain the significant shift of T_g towards higher values. The decrease of the molecular mobility should lead to an increase of the barrier properties of the coating. This point will be discussed later based on electrochemical impedance spectroscopy data. It is noteworthy that the intensity of the peak was higher for the epoxy coating containing IBA-modified clay. This could be attributed to the presence of water molecules in the clay backbone which increased the conductivity. The presence of water in the clay platelets was clearly shown by the thermodegradation curves (Fig. 3).

FE-SEM micrographs of the fracture surface of the epoxy coating containing 2% IBA-modified clay are shown in Fig. 5. It can be seen in Fig. 5a that a rough fracture surface occurs and caused by shear deformation in the presence of IBA-modified clay. Similar micrographs were recently presented by Zhou et al. [21]. In our case, agglomerated particles were also observed. Fig. 5b shows the high magnification micrograph of the clay agglomeration. The silicate layers (lamellar structure) appeared uniformly embedded in the epoxy resin indicating that the polymer penetrated through the platelets. The micrographs revealed the heterogeneous structure of the system. It is
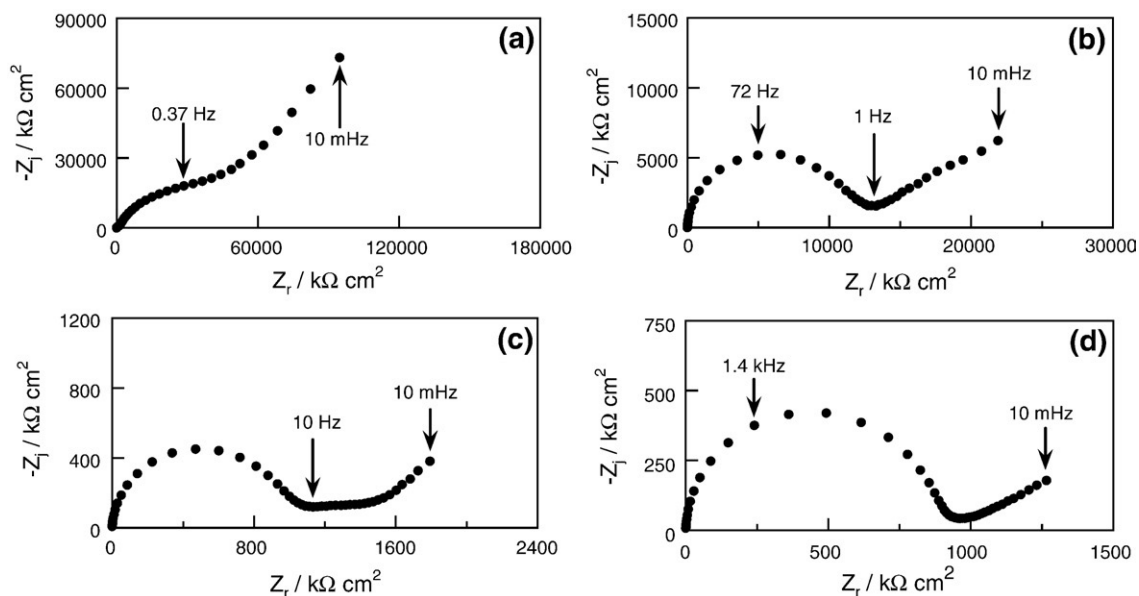

Fig. 6. Electrochemical impedance diagrams obtained for the carbon steel covered by the pure epoxy coating after (a) 7 days, (b) 35 days, (c) 70 days and (d) 140 days of exposure to 0.5 M NaCl solution.
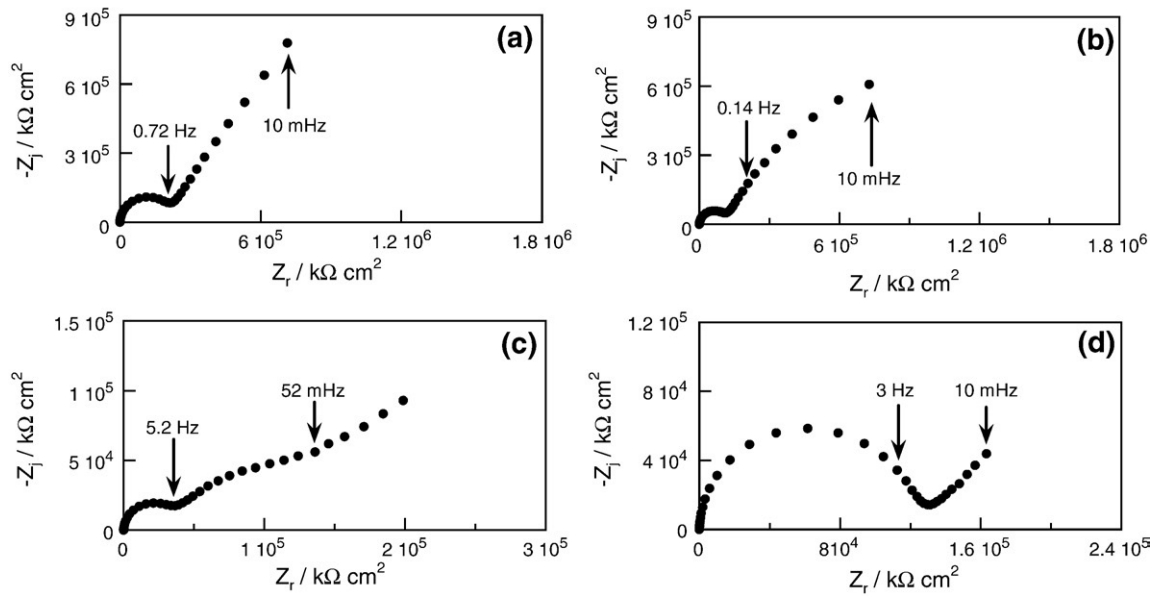
Fig. 7. Electrochemical impedance diagrams obtained for the carbon steel covered by the epoxy coating containing 2 wt.% IBA-modified clay after (a) 7 days (b) 35 days, (c) 70 days and (d) 140 days of exposure to 0.5 M NaCl solution.

obvious that IBA-modified clay was dispersed in the epoxy coating but the presence of some aggregates in different places through the coating underlines that the dispersion and more specifically the exfoliation of the platelets in the coating was not fully completed. The dispersion of layered silicate is an important parameter which is controlled during preparation of the epoxy mixture [22]. Improved dispersion of the clay layers in the organic coating will constitute an interesting development for further studies in corrosion protection.

3.2. Electrochemical impedance results

Impedance diagrams were plotted at the corrosion potential to characterize the corrosion resistance of the carbon steel covered by the pure epoxy coating and by the epoxy coating containing 2% IBA-modified clay. As an example, the impedance diagrams, plotted after four different exposure times in the 0.5 M NaCl solution, are presented in Figs. 6 and 7 for the pure epoxy coating and the epoxy coating containing 2% IBA-modified clay, respectively. For organic coatings, the usual interpretation of the impedance diagrams is the following: the high-frequency (HF) part is related to the organic coating while the low-frequency (LF) part corresponds to the reactions occurring on the metal through defects and pores in the coating [23,24]. For the pure epoxy coating, before 70 days (Fig. 6a and b), a linear part appeared in the LF range, which suggests that diffusion processes occur through the coating [25]. From 70 days of exposure to the NaCl solution, a third time constant appeared in the medium frequency range (Fig. 6c). This behaviour, coupled with the decrease of the impedance value, is due to the degradation of the system. The modification of the LF part of the diagram can be attributed to the presence of corrosion products at the steel/coating interface. As a matter of fact, brown rusty corrosion products are clearly visible under the coating after 70 days of exposure. For the epoxy coating containing 2% of IBA-modified clay (Fig. 7(a–d)), the impedance diagrams also presented different shapes depending on the immersion time. During the first 35 days, the LF part of the diagrams is linear. After 35 days of exposure, the HF loop decreases slightly and the second capacitive loop is better defined. Then, after 70 days of exposure, as in the previous case for the pure epoxy coating, a distinct new time constant appears in the medium frequency range. This loop accounts for the processes occurring at

the carbon steel/coating interface. However, in this case, no corrosion products appeared under the coating. After 140 days of exposure, the diagrams are characterized in the LF part by a straight line (Warburg character) and the total impedance remained high. For the epoxy coating with IBA-modified clay, the impedance values are significantly higher than those obtained for pure epoxy.

The values of the resistance associated with the HF loop (R_f), extracted from the impedance diagrams by a fitting procedure, were used to follow the degradation of the two systems with exposure time in the aggressive solution. R_f is associated with ionic transport through the coating and thus, gives information on the barrier properties of the coating. Fig. 8 reports the variation of R_f as a function of exposure time in the aggressive solution. For the pure epoxy coating, R_f decreased during the first 50 days of immersion and then remained relatively stable with immersion time at around 10^3 kΩ cm^2. A rapid decrease of R_f was observed during the first 10 days of immersion. For the epoxy coating containing IBA-modified clay, the same features were observed. However, the values of R_f are
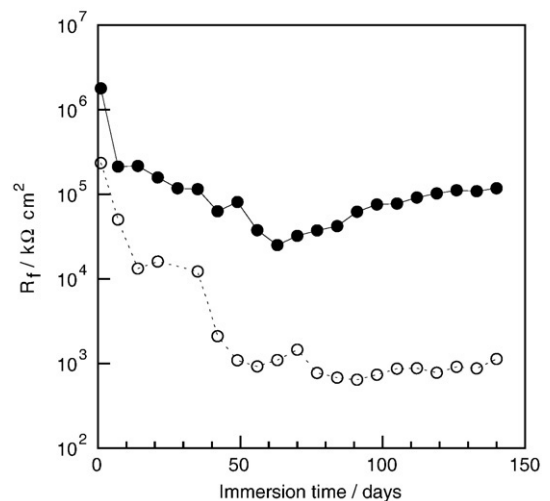

Fig. 8. R_f versus immersion time in 0.5 M NaCl solution for the carbon steel covered by (○) pure epoxy and (●) epoxy containing 2 wt.% IBA-modified clay.
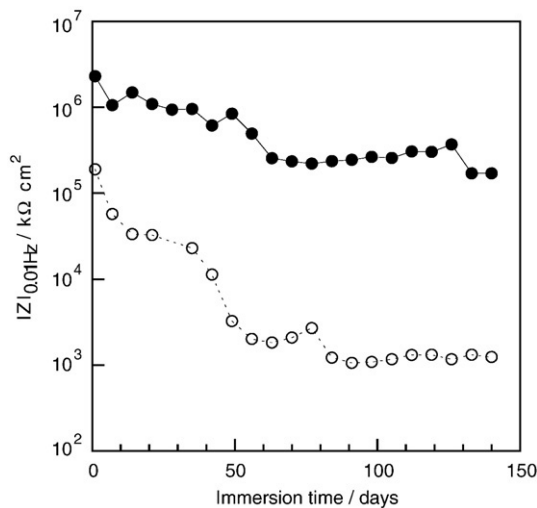
Fig. 9. $|Z|_{0.01\ Hz}$ versus immersion time in 0.5 M NaCl solution for the carbon steel covered by (○) pure epoxy and (●) epoxy containing 2 wt.% IBA-modified clay.

significantly higher and the decrease of R_f during the first 60 days is less marked indicating that the introduction of the clay particles in the epoxy coating led to a significant improvement of the barrier properties. This result is in agreement with the TSC data which have shown that the IBA-modified clay decreases the molecular mobility of the coating by comparison with the pure epoxy. After 60 days of exposure, the R_f value increased slightly with increasing immersion time. This could be attributed to different phenomena such as the decrease of pore number, the decrease of the pore size or pore sealing at the steel/coating interface. These phenomena are linked to the presence of IBA-modified clay in the coating.

The LF part of the diagrams is not well defined (Figs. 6 and 7) and consequently the parameters associated with the corrosion processes (charge transfer resistance and double layer capacitance) cannot be readily extracted. Nevertheless, it was proposed by Kittel et al. [26] and the group of Bierwagen [27–29] that the impedance modulus at low frequencies (such as $|Z|_{1\ Hz}$ or $|Z|_{0.01\ Hz}$) measured versus exposure time could serve as an estimation of the corrosion protection of a painted metal. Fig. 9 shows the evolution of $|Z|_{0.01\ Hz}$ with immersion time in the 0.5 M NaCl solution for the carbon steel covered by pure epoxy and epoxy containing 2% of IBA-modified clay. The same pattern
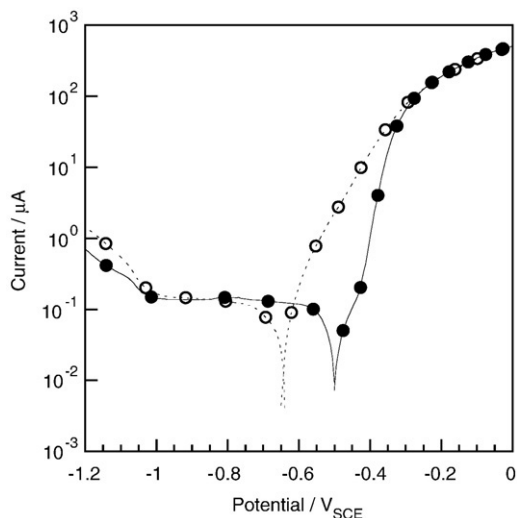
was obtained by plotting $|Z|_{1\ Hz}$ versus exposure time. For both systems, the impedance modulus decreased during the first 60–70 days of immersion but the decrease was less strong with IBA-modified clay. For the pure epoxy coating, the modulus remained stable after 80 days of exposure. For the coating containing IBA-modified clay, the modulus slightly increased between 60 and 140 days of exposure reaching a value about 200 times higher than that measured without clay. These results clearly show that the addition of IBA-modified clay markedly improved the corrosion resistance of the carbon steel.

The inhibitor concentration in the film was relatively low (10% of IBA introduced in the clay and only 2% of IBA-modified clay dispersed in the epoxy coating). To define the role of IBA at the steel/coating interface, an artificial defect was made in both coatings. For comparison, polarization curves obtained for the two systems are presented in Fig. 10. For the IBA-modified clay coating, a shift of the corrosion potential towards more positive values (150 mV) and lower current densities can be seen by comparison with the pure epoxy system. This corroborates the anodic inhibition effect of IBA and shows that IBA molecules are available at the interface to inhibit the corrosion of carbon steel [12]. However, it is not clearly established how the molecules reach the metal surface. IBA can be released with water from the clay through the coating or can already be present at the interface due to its migration during epoxy drying.

From the electrochemical measurements, it can be concluded that the IBA-modified clay both plays a role on the barrier effect of the
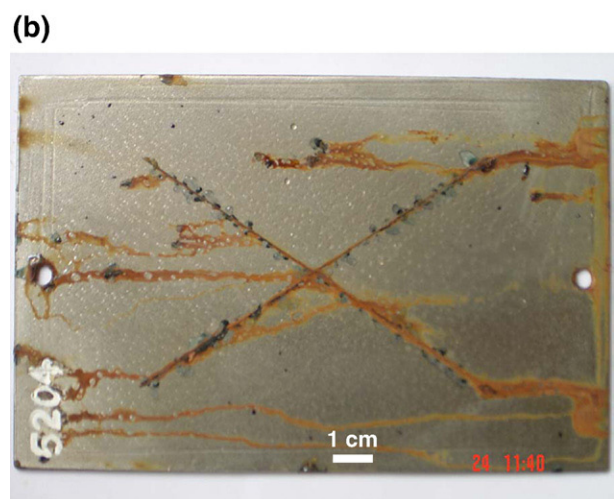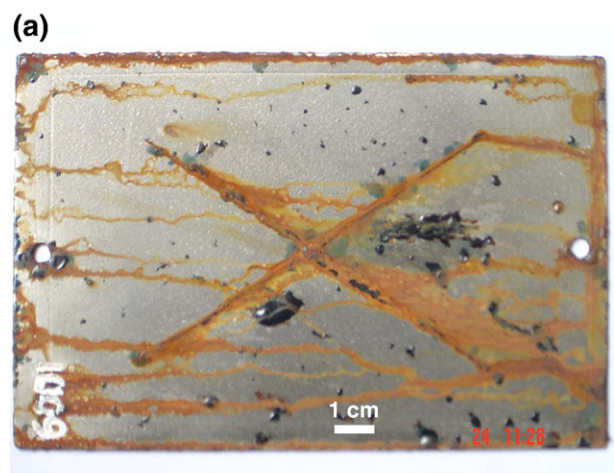

(a)

Fig. 10. Polarization curves measured in the presence of an artificial defect for carbon steel covered by (○) pure epoxy and (●) epoxy containing 2 wt.% IBA-modified clay.

(b)

Fig. 11. Photographs of sheet steel with (a) pure epoxy and (b) epoxy containing 2 wt.% IBA-modified clay after 35 days of exposure in the salt spray chamber (ASTM 1654).

coating and also acts as a corrosion inhibitor at the carbon steel/coating interface.

Finally, salt spray test was used to evaluate the performance of the carbon steel covered by the pure epoxy coating and the epoxy coating containing 2% IBA-modified clay following ASTM 1654. After the exposure of the two systems for 840 h (35 days) some differences were observed on and around scratches made on the surface of the samples (Fig. 11). For the pure epoxy coating (Fig. 11a), numerous blisters (black corrosion products) were observed near the scratch with some scattered over the whole coating surface. Moreover, brown, rusty and poorly adherent corrosion products accumulated on the scribe. For the epoxy coating with IBA-modified clay (Fig. 11b), the blisters were noted essentially around the scribe. The brown, rusty, poorly adherent corrosion products are generally described as a mixture of iron hydroxides [30] whereas the black and more adherent corrosion products are identified as conducting magnetite [30]. Delamination around the scratches was limited for the epoxy coating with IBA-modified clay indicating the relatively good adherence of the coating. Adherence, evaluated following the standard ASTM 3359 (not reported here), was found to be acceptable. The salt spray test confirmed the good corrosion protection afforded by the coating containing the IBA-modified clay.

4. Conclusions

The corrosion protection of carbon steel by an epoxy resin containing IBA-modified clay was investigated by electrochemical impedance spectroscopy. It was shown that the barrier properties of the epoxy coating were significantly higher in the presence of IBA-modified clay by comparison with the pure epoxy. The lamellar structure of the clay (separated platelets in the epoxy matrix) and the electrostatic interactions between silicate layers and the epoxy resin made the coating more impermeable (higher T_g value) which explains that the barrier effect is improved. Although only a small proportion of IBA was incorporated into the coating, high corrosion protection was afforded. In the presence of a defect, the inhibitive action of the IBA was clearly shown at the carbon steel/epoxy coating interface. By comparison with the previous study, the adherence of the coating was better which constitutes major progress. FE-SEM revealed the existence of layered clay agglomerates. It will be necessary to improve the dispersion of the clay platelets in the coating during resin preparation and to evaluate the influence of this parameter on coating performance.

The present study confirms the feasibility of developing new formulations without toxic inhibitors.

References

[1] Y. Yamamoto, H. Nishihara, K. Aramaki, Corrosion 48 (1992) 641.
[2] N. Ochoa, F. Moran, N. Pébère, B. Tribollet, Corros. Sci. 47 (2005) 593.
[3] M. Lebrini, F. Bentiss, H. Vezin, M. Lagrenee, Corros. Sci. 48 (2006) 1279.
[4] El Sayed H. El Ashry, Ahmed El Nemr, Sami A. Esawy, Safaa Ragab, Electrochim. Acta 51 (2006) 3957.
[5] H. Amar, A. Tounsi, A. Makayssi, A. Derja, J. Benzakour, A. Outzourhit, Corros. Sci. 49 (2007) 2936.
[6] S. Bohm, H.N. McMurray, S.M. Powell, D.A. Worsley, Mater. Corros. 52 (2001) 896.
[7] R.B. Leggat, S.A. Taylor, S.R. Taylor, Colloids Surf., A Physicochem. Eng. Asp. 210 (2002) 83.
[8] R.G. Buchheit, H. Guan, S. Mahajanam, F. Wong, Prog. Org. Coat. 47 (2003) 174.
[9] T. Sugama, Mater. Lett. 60 (2006) 2700.
[10] S.-A. Garea, H. Iovu, Prog. Org. Coat. 56 (2006) 319.
[11] T.X.H. To, A.T. Trinh, H.N. Truong, O.K. Vu, J.-B. Jorcin, N. Pébère, Surf. Coat. Technol. 201 (2007) 7408.
[12] A.T. Trinh, L.T. Dao, T.X.H. To, Proceedings of the 14th Asian–Pacific Corrosion Control Conference, Shanghai, China, 2006.
[13] C. Corfias, N. Pébère, C. Lacabanne, Corros. Sci. 41 (1999) 1539.
[14] C. Corfias, N. Pébère, C. Lacabanne, Corros. Sci. 42 (2000) 1337.
[15] C. Le Pen, C. Lacabanne, N. Pébère, Prog. Org. Coat. 39 (2000) 167.
[16] C. Le Pen, C. Lacabanne, N. Pébère, Prog. Org. Coat. 46 (2003) 77.
[17] J. Madejová, Vibr. Spectrosc. 31 (2003) 1.
[18] R.O. Carter III, C.A. Gierczak, R.A. Dickie, Appl. Spectrosc. 40 (1986) 649.
[19] K.A. Carrado, Appl. Clay Sci. 17 (2000) 1.
[20] F.M. Uhl, S.P. Davuluri, S.-C. Wong, D.C. Webster, Polymer 45 (2004) 6175.
[21] Y. Zhou, F. Pervin, M.A. Biswas, V.K. Rangari, S. Jeelani, Mater. Lett. 60 (2006) 869.
[22] J. Langat, S. Bellayer, P. Hudrlik, A. Hudrlik, P.H. Maupin, J.W. Gilman Sr., D. Raghavan, Polymer 47 (2006) 6698.
[23] L. Beaunier, I. Epelboin, J.C. Lestrade, H. Takenouti, Surf. Technol. 41 (1976) 237.
[24] N. Pébère, T. Picaud, M. Duprat, F. Dabosi, Corros. Sci. 29 (1989) l073.
[25] L. Jianguo, G. Gaoping, Y. Chuanwei, Electrochim. Acta 50 (2005) 3320.
[26] J. Kittel, N. Celati, M. Keddam, H. Takenouti, Prog. Org. Coat. 46 (2003) 135.
[27] G.P. Bierwagen, D. Tallman, J. Li, L. He, C. Jeffcoate, Prog. Org. Coat. 46 (2003) 148.
[28] R.L. De Rosa, D.A. Earl, G.P. Bierwagen, Corros. Sci. 44 (2002) 1607.
[29] B.R. Hinderliter, S.G. Croll, D.E. Tallman, Q. Su, G.P. Bierwagen, Electrochim. Acta 51 (2006) 4505.
[30] T. Missawa, K. Hashimoto, S. Shimodaira, Corros. Sci. 14 (1974) 131.